New Journal of Physics
The open access journal at the forefront of physics

Deutsche Physikalische Gesellschaft DPG IOP Institute of Physics

PAPER

Polarization-sensitive absorption of THz radiation by interacting electrons in chirally stacked multilayer graphene

To cite this article: Maxim Trushin and John Schliemann 2012 *New J. Phys.* **14** 095005

New Journal of Physics
The open-access journal for physics

Polarization-sensitive absorption of THz radiation by interacting electrons in chirally stacked multilayer graphene

Maxim Trushin[1] **and John Schliemann**
Institute for Theoretical Physics, University of Regensburg,
D-93040 Regensburg, Germany
E-mail: maxim.trushin@physik.uni-regensburg.de

New Journal of Physics **14** (2012) 095005 (10pp)
Received 8 February 2012
Published 10 September 2012
Online at http://www.njp.org/
doi:10.1088/1367-2630/14/9/095005

Abstract. We show that the opacity of a clean multilayer graphene flake depends on the helicity of the circular polarized electromagnetic radiation. The effect can be understood in terms of the pseudospin selection rules for the interband optical transitions in the presence of exchange electron–electron interactions which alter the pseudospin texture in momentum space. The interactions described within a semi-analytical Hartree–Fock approach lead to the formation of topologically different broken symmetry states characterized by Chern numbers and zero-field anomalous Hall conductivities.

Contents

[1] Author to whom any correspondence should be addressed.

1. Introduction

Multilayer graphene is a link between one atom thick carbon layers [1] with the peculiar Dirac-like effective Hamiltonian for carriers [2] and graphite [3], which can be seen as millions of graphene layers stacked together. Graphene layers placed together do not lie exactly one on top of each other but are shifted in such a way that only half of the carbon atoms have a neighbor in another layer and the other half are projected right into the middle of the graphene's 'honeycomb cell'. If the third layer aligns with the first (and the $n+2$ layer with the nth), then we arrive at a more stable arrangement of graphene layers known as the Bernal (or AB) stacking, see figure 1(a). However, this is not the only possible configuration. One can imagine an alternative stacking when the third layer aligns with neither the first nor the second but is shifted with respect to both, see figure 1(b). This arrangement is known as rhombohedral (or ABC) stacking and is the main topic of this work.

The very first studies of Bernal and rhombohedral graphites [3–7] relying on the tight binding model have demonstrated the strong dependence of the band structure on stacking order. Later on, progress in numerical methods made it possible to refine the tight binding model outcomes using *ab initio* calculations [8–10]. The seminal transport measurements on graphene [11] have inspired recent investigations [12–16] on the band structure in a few-layer graphene having different stacking patterns. The band structure demonstrates a large variety of behaviors including a gapless spectrum, direct and indirect band gaps and energetic overlap of the conduction and valence bands even though the number of layers has been limited to four [12]. Note that the band gap can be induced by an external electric field [16]. The influence of an external magnetic field (Landau levels) has also been studied extensively [15, 17, 18]. The electron–electron interactions have been taken into account in [19–23], including the Zeeman term [24]. There are experimental indications that electron–electron interaction effects play an important role in a few-layer graphene where charge carriers may exhibit a variety of broken symmetry states [25–28].

The brief literature review given above illustrates how rich the band structure of multilayer graphene (and the effects associated with it) can be. Note, however, that among all stacking possibilities, only the pure ABC arrangement maintains the sublattice pseudospin chirality [29]. In the simplest case of negligible interlayer asymmetries and trigonal warp the simplified two-band ABC graphene model leads to the following Hamiltonian close to the neutrality point [29]:

$$H_0^{\nu} = \frac{(\hbar v_0)^N}{(-\gamma_1)^{N-1}} \begin{pmatrix} 0 & (\nu k_x - \mathrm{i}k_y)^N \\ (\nu k_x + \mathrm{i}k_y)^N & 0 \end{pmatrix}, \tag{1}$$

where $v_0 \approx 10^6\,\mathrm{ms}^{-1}$ is the group velocity for carriers in single-layer graphene, γ_1 is the hopping parameter, $\nu = \pm$ is the valley index and N is the number of layers. As one can see from equation (1), the N-layer and $(N+1)$-layer graphene stacks differ, apart from the density of states, by only the winding number associated with the pseudospin orientation. The pseudospin texture in the momentum space associated with Hamiltonian (1) and shown in figure 2 is the main topic of this work. In what follows, we focus on the influence of electron–electron exchange interactions on the pseudospin texture and its detection by optical means.

Note that the pseudospin lies in the xy-plane as long as its carrier remains in an eigenstate of H_0^{ν}. The exchange interactions can turn the pseudospin texture into the out-of-plane phase with the out-of-plane angle depending on the absolute value of the particle momentum [21, 30–32]. This is due to the huge negative contribution to the Hartree–Fock ground state energy

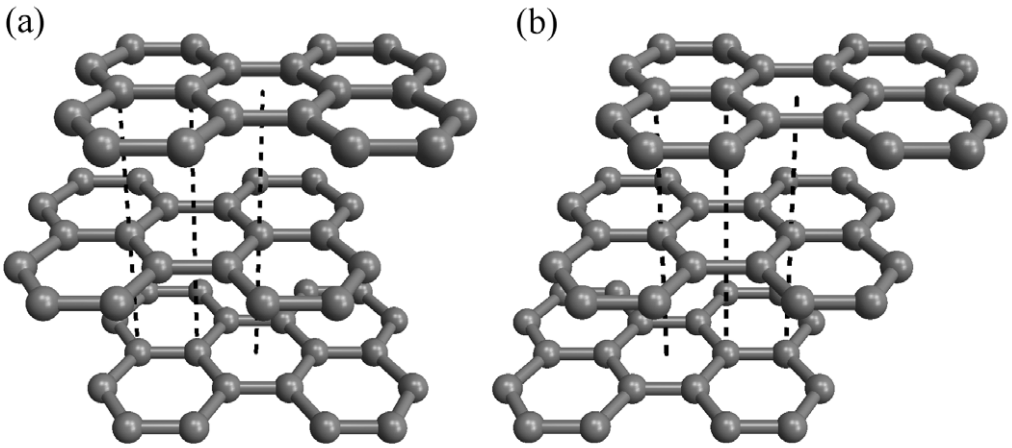

Figure 1. (a) Bernal graphite represents graphene layers placed together in ···-AB-AB-AB-··· stacking when the two layers shifted with respect to each other by 0.142 nm alternate in bulk. (b) Rhombohedral graphite requires three non-equivalent graphene layers when the two layers are shifted with respect to the first one by 0.142 and 0.284 nm alternating in ···-ABC-ABC-ABC-··· sequence. Dashed lines are a guide to the eye. Note that only ···-ABC-··· stacking order results in the effective Hamiltonian (1) employed in this paper.

from the valence band (i.e. 'antiparticle' states), which cannot be neglected in graphene because of the zero gap and conduction–valence band coupling via pseudospin. The broken symmetry states in multilayer graphene with chiral stacking have recently been studied by Zhang *et al* [21] using quite general arguments. Spontaneous symmetry breaking can occur in the presence of exchange electron–electron interactions [32]. Here, we utilize a simplified model which includes exchange electron–electron interactions but, at the same time, allows transparent half-analytical solutions. Having this solution at hand we focus on the manifestation of such broken symmetry states in optical absorption measurements.

Optical absorption via the direct interband optical transitions in monolayer graphene has been investigated in [33] and shown to be equal to the universal value $\pi e^2/\hbar c$. In the presence of the electron–electron interactions, the interband absorption can be substantially reduced or enhanced as compared with its universal value $\pi e^2/\hbar c$ just by switching the helicity of the circularly polarized light [30]. This effect is due to the peculiar pseudospin texture arising from the interplay between pseudospin–momentum coupling and exchange interactions. To observe the pseudospin texture in chirally stacked multilayer graphene by optical means the photon energy must be much smaller than the bottom of the lowest split-off bands $\gamma_1 = 0.4\,\mathrm{eV}$. To give an example, a CH_3OH 20 mW laser [34] with wavelength 118 μm (i.e. with an photon energy of 10.5 meV) safely satisfies this condition.

2. Model

We start from the Coulomb exchange Hamiltonian for chiral carriers, which is given by

$$H^{\nu}_{\mathrm{exch}}(\mathbf{k}) = -\sum_{\kappa'} \int \frac{\mathrm{d}^2 k'}{4\pi^2} U_{|\mathbf{k}-\mathbf{k}'|} |\chi^{\nu}_{k'\kappa'}\rangle\langle\chi^{\nu}_{k'\kappa'}| \tag{2}$$

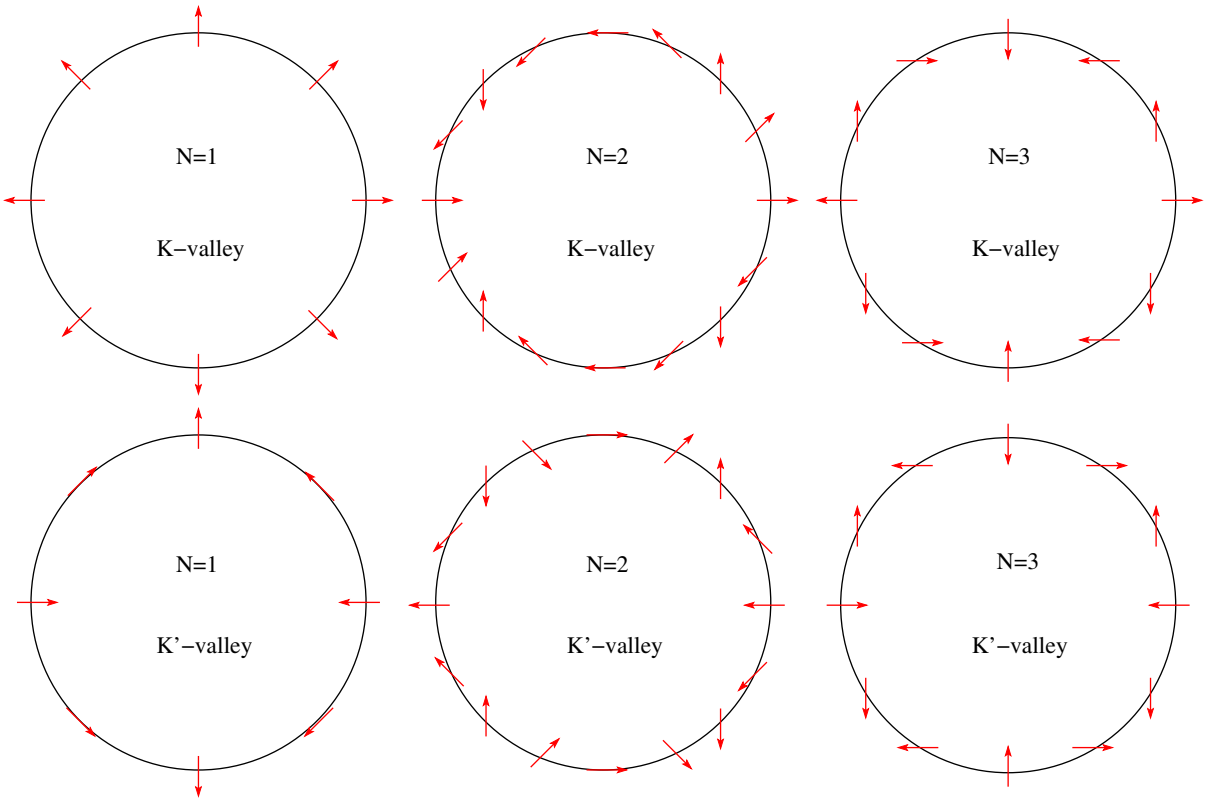

Figure 2. Top view of the pseudospin texture for the conduction band in chirally stacked multilayer graphene calculated from the non-interacting Hamiltonian (1). The pseudospin orientations in conduction and valence bands for a given momentum are antiparallel.

with $U_{|\mathbf{k}-\mathbf{k}'|} = 2\pi e^2/\varepsilon|\mathbf{k}-\mathbf{k}'|$ and $\kappa' = \pm$ being the band index with $\kappa = +$ for the conduction band. In order to consider the exchange Hamiltonian for any N on an equal footing, we assume a strictly two-dimensional (2D) Fourier transform for the Coulomb potential. This is in contrast to [32], where the interlayer distance $d = 0.335$ nm has been included in the screening multiplier $\exp(-|\mathbf{k}-\mathbf{k}'|d)$. Since the wave vector difference $|\mathbf{k}-\mathbf{k}'|$ cannot be larger than the momentum cut-off of the order of 10^7 cm^{-1} employed in our model (see below), the screening multiplier is always of the order of 1 and can be disregarded here. The intervalley overlap is also assumed to be negligible, and the eigenstates of $H^\nu = H_0^\nu + H_{\rm exch}^\nu$ can be formulated as $\Psi_{\mathbf{k}\kappa}^\nu(\mathbf{r}) = e^{i\mathbf{kr}}|\chi_{k\kappa}^\nu\rangle$ with spinors $|\chi_{k+}^\nu\rangle = (\cos\frac{\vartheta_k}{2}, \nu\sin\frac{\vartheta_k}{2}e^{\nu Ni\varphi})^{\rm T}$, $|\chi_{k-}^\nu\rangle = (\sin\frac{\vartheta_k}{2}, -\nu\cos\frac{\vartheta_k}{2}e^{\nu Ni\varphi})^{\rm T}$, and $\tan\varphi = k_y/k_x$, where a nonzero out-of-plane pseudospin component corresponds to $\vartheta_k \neq \pi/2$. To diagonalize H^ν, the following ν-independent equation for ϑ_k must be satisfied [30, 35]:

$$\frac{(\hbar v_0 k)^N}{(-\gamma_1)^{N-1}}\cos\vartheta_k + \sum_{\kappa'}\int\frac{d^2k'}{8\pi^2}\kappa' U_{|\mathbf{k}-\mathbf{k}'|}\left[\cos\vartheta_{k'}\sin\vartheta_k - \sin\vartheta_{k'}\cos\vartheta_k\cos(N\varphi' - N\varphi)\right] = 0. \tag{3}$$

Here the integration goes over the occupied states. Note that the conduction and valence states are entangled, and the latter cannot be disregarded even at the positive Fermi energies assumed below. Thus, in order to evaluate the integrals in equation (3) a momentum cut-off Λ is

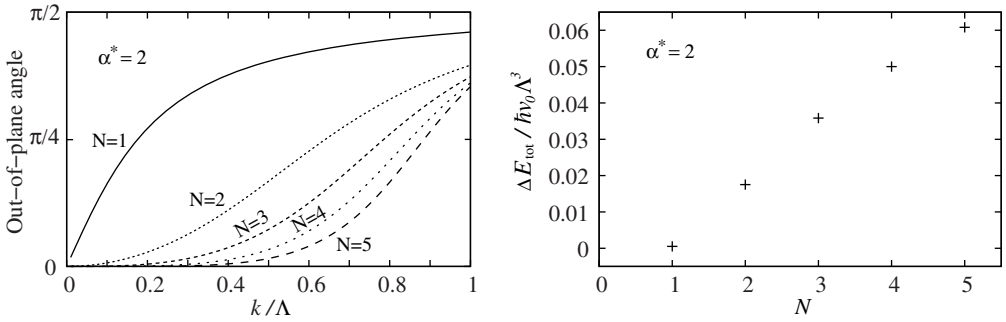

Figure 3. Left panel: the pseudospin out-of-plane angle $\vartheta(k)$ for substrate-free chirally stacked N-layer graphene numerically calculated from equation (4). Right panel: the total ground state energy difference (5) between the in-plane and out-of-plane phases for different N. Increasing N makes the out-of-plane phase more preferable. The $\vartheta(k)$ curve for $N = 1$ differs from the one given in [30] since we have improved the precision of our calculations here. Note that the Coulomb interactions are completely unscreened here. The screening is taken into account in figure 4 by introducing the effective dielectric constant ε which relates to α^* as $\alpha^* = e^2/(\varepsilon\hbar v_0)$.

necessary. The most natural choice $\Lambda = \gamma_1/\hbar v_0$ corresponds to the energy scale γ_1 at which the split-off bands of bilayer graphene become relevant and our two-band model no longer applies. Substituting $x = k/\Lambda$ we arrive at

$$\frac{4\pi}{\alpha^*} x^N \cos\vartheta_k = \int_0^{2\pi} \mathrm{d}\varphi' \int_{k_F/\Lambda}^1 \mathrm{d}x' x' \frac{\cos\vartheta_{k'} \sin\vartheta_k - \sin\vartheta_{k'} \cos\vartheta_k \cos N\varphi'}{\sqrt{x^2 + x'^2 - 2xx' \cos\varphi'}}, \tag{4}$$

where $\alpha^* = e^2/(\varepsilon\hbar v_0)$. The momentum cut-off is assumed to be much larger than the Fermi momentum k_F and, therefore, we can set the lower integral limit to zero. In this case our outcomes do not depend on the value of Λ.

Besides a trivial solution with $\vartheta_0 = \pi/2$ independent of k, there are nontrivial ones $\vartheta_1 = \vartheta(k)$ and $\vartheta_2 = \pi - \vartheta(k)$ with $\vartheta(k)$ shown in figures 3(a) and 4(a) for different N and α^*. The solutions ϑ_0 and $\vartheta_{1,2}$ represent two phases with different total ground state energies $E_{\mathrm{tot}}^{\mathrm{in}}$ ($E_{\mathrm{tot}}^{\mathrm{out}}$) for the in-plane (out-of-plane) pseudospin phase. The difference $\Delta E_{\mathrm{tot}} = E_{\mathrm{tot}}^{\mathrm{in}} - E_{\mathrm{tot}}^{\mathrm{out}}$ per volume is given by

$$\frac{\Delta E_{\mathrm{tot}}}{\hbar v_0 \Lambda^3} = -\frac{g_s g_v}{2\pi} \int_0^1 \mathrm{d}x' x'^{N+1} (1 - \sin\vartheta_{k'}) - \alpha^* \frac{g_s g_v}{32\pi^3} \int_0^{2\pi} \mathrm{d}\varphi \int_0^{2\pi} \mathrm{d}\varphi' \int_0^1 \mathrm{d}x \int_0^1 \mathrm{d}x' \times xx' \frac{(1 - \sin\vartheta_{k'} \sin\vartheta_k)\cos(N\varphi' - N\varphi) - \cos\vartheta_{k'} \cos\vartheta_k}{\sqrt{x^2 + x'^2 - 2xx' \cos(\varphi - \varphi')}}. \tag{5}$$

The ground state energy is the same for *both* valleys and spins and, therefore, equation (5) contains $g_s = 2$ and $g_v = 2$ for spin and valley degeneracy, respectively. ΔE_{tot} has been evaluated numerically and the resulting ΔE_{tot} versus N dependence is shown in figures 3(b) and 4(b) for suspended and SiO_2-placed graphene, respectively. One can see that strong electron–electron interactions with $\alpha^* = 2$ definitely make the out-of-plane phase energetically preferable for $N > 1$. For graphene placed on SiO_2 substrate the pseudospin out-of-plane phase

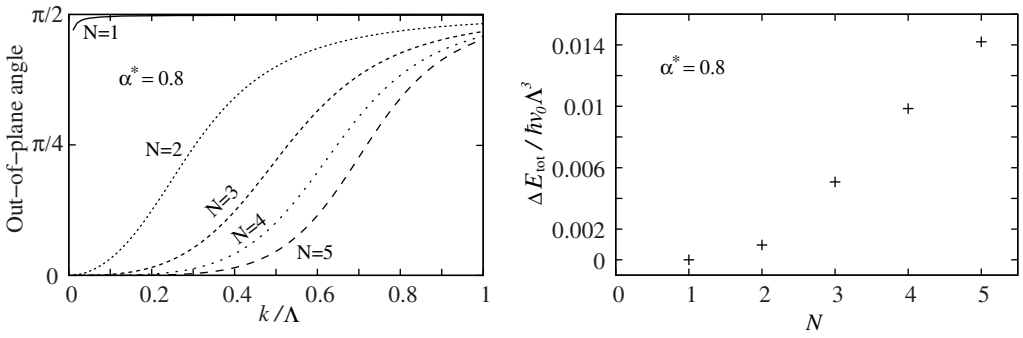

Figure 4. Left panel: the pseudospin out-of-plane angle $\vartheta(k)$ for chirally stacked N-layer graphene on SiO_2 numerically calculated from equation (4). Right panel: the total ground state energy difference (5) between the in-plane and out-of-plane phases for different N. The difference is much larger in the case of substrate-free graphene, see figure 3.

is energetically preferable only for $N \geqslant 3$. Note that the estimates of α^* for clean monoatomic graphene flake vary from 2 ([36]) to 2.8 ([37]) and, therefore, even monolayer graphene may get to the pseudospin out-of-plane phase.

Note that it is possible to choose either the same or opposite solutions for two valleys. The former choice breaks the parity invariance, whereas the latter one does so with the time reversal symmetry [30]. In what follows, we consider possible manifestations of these solutions in the optical absorption measurements on multilayer graphene.

3. Optical absorption

We assume that an electromagnetic wave is propagating along the z-axis perpendicular to the graphene plane. It can be described by the electric field $\mathbf{E} = \mathbf{E}_0 \exp(\mathrm{i}k_z z - \mathrm{i}\omega t)$, where k_z is the wave vector and ω is the radiation frequency. For our purpose, it is more convenient to characterize the electromagnetic wave by its vector potential $\mathbf{A} = \mathbf{A}_0 \exp(\mathrm{i}k_z z - \mathrm{i}\omega t)$, where $\mathbf{A}_0 = \mathrm{i}c\mathbf{E}/\omega$. The relation between $\mathbf{E}$ and $\mathbf{A}$ is unambiguous since $\mathbf{A}$ is always in the xy-plane, resulting in a gauge with $\operatorname{div}\mathbf{A} = 0$. The interaction Hamiltonian can then be written in the lowest order in $\mathbf{A}$ as

$$H_{\mathrm{int}}^{\nu} = \frac{(\nu\hbar v_0 k)^N}{k(-\gamma_1)^{N-1}} \frac{eN}{\hbar c} \begin{pmatrix} 0 & \mathrm{e}^{-\nu \mathrm{i}\varphi(N-1)}(A_x - \mathrm{i}\nu A_y) \\ \mathrm{e}^{\nu \mathrm{i}\varphi(N-1)}(A_x + \mathrm{i}\nu A_y) & 0 \end{pmatrix}. \tag{6}$$

The total absorption P can be calculated as a ratio between the total electromagnetic power absorbed by graphene per unit square $W_{\mathrm{a}} = \hbar\omega \sum_{\nu} \int \frac{\mathrm{d}^2 k}{4\pi^2} w(\mathbf{k}+, \mathbf{k}-)$ and the incident energy flux $W_{\mathrm{i}} = \omega^2 A^2 / 4\pi c$. The probability to excite an electron from the valence band to an unoccupied state in the conduction band $w(\mathbf{k}+, \mathbf{k}-)$ can be calculated using Fermi's golden rule

$$w(\mathbf{k}+, \mathbf{k}-) = \frac{2\pi}{\hbar} |\langle \mathbf{k}+ | H_{\mathrm{int}}^{\nu} | \mathbf{k}- \rangle|^2 \delta(E_{k+} - E_{k-} - \hbar\omega).$$

Because of normal incidence there is zero momentum transfer from photons to electrons. What is important is that the interband transition matrix elements of H_{int}^{ν} turn out to be sensitive to

the light polarization and pseudospin orientations in the initial and final states. In particular, for linear polarization with $A_x = A\cos\varphi_{\rm pol}$ and $A_y = A\sin\varphi_{\rm pol}$ the probability of exciting an electron with a given momentum reads

$$w(\mathbf{k}+,\mathbf{k}-)|_{\nu=+} = \frac{\pi}{\hbar}\left(\frac{eN}{\hbar c}A\right)^2 \frac{(\hbar v_0)^{2N}k^{2N-2}}{(-\gamma_1)^{2N-2}}\delta(E_{k+}-E_{k-}-\hbar\omega) \times\left[1+\cos^2\vartheta_k-\sin^2\vartheta_k\cos(2\varphi-2\varphi_{\rm pol})\right]. \tag{7}$$

Note that $w(\mathbf{k}+,\mathbf{k}-)$ does not depend on the valley index ν. The total optical absorption P is not sensitive to the particular orientation of the polarization plane since the $\varphi_{\rm pol}$-dependent term is integrated out in this case. In contrast, if we assume a circular polarization fulfilling $A_x = \pm iA/\sqrt{2}$, $A_y = A/\sqrt{2}$, then the interband transition probability for K-valley can be written as

$$w(\mathbf{k}+,\mathbf{k}-)|_{\nu=+} = \frac{4\pi}{\hbar}\left(\frac{eN}{\hbar c}A\right)^2 \frac{(\hbar v_0)^{2N}k^{2N-2}}{(-\gamma_1)^{2N-2}}\begin{Bmatrix}\sin^4\frac{\vartheta_k}{2}\\ \cos^4\frac{\vartheta_k}{2}\end{Bmatrix}\delta(E_{k+}-E_{k-}-\hbar\omega). \tag{8}$$

Here, the multipliers $\sin^4(\vartheta_k/2)$ and $\cos^4(\vartheta_k/2)$ are for two opposite helicities of light, and for K′-valley they are interchanged. If the out-of-plane pseudospin polarization is chosen to be opposite in two valleys, then this helicity dependence survives the integration over momentum and summation over the valley index, resulting in the helicity-sensitive total absorption which reads

$$P = \frac{16N^2}{\hbar\omega}\frac{\pi e^2}{\hbar c}\frac{(\hbar v_0)^{2N}}{(-\gamma_1)^{2N-2}}\int_0^\Lambda dk k^{2N-1}\begin{Bmatrix}\sin^4\frac{\vartheta_k}{2}\\ \cos^4\frac{\vartheta_k}{2}\end{Bmatrix}\delta(E_{k+}-E_{k-}-\hbar\omega). \tag{9}$$

The absorption strongly depends on helicity as long as the radiation frequency is much smaller than the band split-off energy. This regime corresponds to the excitation of electrons with comparatively small momenta, where the angle ϑ_k is close to zero, see figures 3(b) and 4(b). In the in-plane phase with $\vartheta_k = \pi/2$ the total absorption does not depend on light polarization, and in the non-interacting limit it is equal to

$$P = N\frac{\pi e^2}{\hbar c}. \tag{10}$$

At $N = 1$ it acquires the universal value $\frac{\pi e^2}{\hbar c}$, as expected [33].

The experiment proposed here is similar to that discussed recently in [38], suggesting to detect broken symmetry states in graphene placed on the substrate by polar Kerr rotation measurements, i.e. by analyzing the elliptical polarization of reflected radiation. In this paper, however, we propose to reach the same goal by comparing the opacity for two orthogonal light polarizations, which appears to be the simpler strategy.

Alternatively, one can characterize broken symmetry states in terms of the topological Chern numbers [39] given by

$$n_\pm^\nu = \frac{1}{2\pi}\int d^2k\nabla_k\times\mathbf{A}_\pm^\nu \tag{11}$$

with $\mathbf{A}_\pm^\nu = i\langle\chi_{k\pm}^\nu|\nabla_k|\chi_{k\pm}^\nu\rangle$. This approach is routinely used in the theory of topological insulators [40] and originated from the description of quantized Hall conductances. A nontrivial band topology has also been found in graphene [41, 42] where the band gap was opened via

spin–orbit coupling characterized just by a constant (i.e. wave vector independent) mass term rather than by exchange interactions described by a more complicated Hamiltonian (2).

Note that in our case here $\nabla_k \times \mathbf{A}_\pm^\nu$ contains a term proportional to $\delta(\mathbf{k})$ which occurs due to the singularity in $\mathbf{A}_\pm^\nu \propto k^{-1}$, but does not contribute to $n_\pm^\nu$ as long as $\vartheta_k = 0$ at $k \to 0$. Thus, for the conduction band electrons we have

$$n_+^\nu = -\frac{\nu N}{2} \int_{\vartheta(0)}^{\vartheta(\Lambda)} \mathrm{d}\vartheta_k \sin\vartheta_k. \tag{12}$$

Assuming the out-of-plane pseudospin polarization to be opposite in two valleys it follows that the total Chern number for conduction electrons just equals N. On the other hand, the total Chern number is zero as long as the out-of-plane pseudospin component is the same in both valleys. Thus, the two out-of-plane solutions are *topologically* different even though they correspond to the band gap of the same size. The topologically nontrivial case with $n \neq 0$ corresponds to broken time reversal symmetry, leading to the existence of a zero-field Hall current [30].

The only question is whether the time reversal broken states really occur in clean graphene samples. A more in-depth analysis performed by Nandkishore and Levitov [22, 38] suggests that this is the case at least for bilayer graphene. On the other hand, Jung *et al* [31] demonstrate that the intervalley exchange coupling favors parallel pseudospin polarization in opposite valleys breaking the parity invariance. In this case, the total absorption does not depend on the radiation helicity but the two valleys are occupied differently by the photoexcited carriers, which might be a useful effect for *valleytronics* [43]. Note that the strain effects may also change the band structure topology in bilayer [44] and probably multilayer graphene. This might be an issue in suspended samples, where mechanical deformations can occur easily. There is, however, experimental evidence [28] for the fact that it is the electron–electron interaction rather than the strain that is responsible for the band structure reconstruction.

4. Conclusion

We have demonstrated that the polarization-sensitive optical absorption predicted in [30] for single-layer graphene can be found in chirally stacked carbon multilayers within a broader range of parameters. This is due to the enhancement of the interaction effects in multilayer graphene with a larger number of layers. The conditions necessary for the observation of the polarization-dependent optical absorption can be summarized as follows. (i) Graphene samples must be prepared as clean as possible. It would be better to utilize suspended samples in order to isolate the interacting electrons from the environment with a large relative permittivity. (ii) The exchange interactions must break the time reversal invariance rather than the parity. This situation corresponds to the topologically nontrivial state with the Chern number equal to N. (iii) Finally, the low-frequency radiation is necessary to excite the electrons with smaller momenta having larger out-of-plane pseudospin components and to preclude the influence of split-off bands.

In addition, we would like to mention the possible existence of a zero-field Hall current in the slightly doped graphene samples where the time reversal invariance is broken as described above.

Acknowledgments

We thank Tobias Stauber, Jeil Jung and Fan Zhang for stimulating discussions. This work was supported by DFG via GRK 1570.

References

[1] Novoselov K S, Geim A K, Morozov S V, Jiang D, Katsnelson M I, Grigorieva I V, Dubonos S V and Firsov A A 2005 Two-dimensional gas of massless Dirac fermions in graphene *Nature* **438** 197
[2] Castro Neto A H, Guinea F, Peres N M R, Novoselov K S and Geim A K 2009 The electronic properties of graphene *Rev. Mod. Phys.* **81** 109–62
[3] Wallace P R 1947 The band theory of graphite *Phys. Rev.* **71** 622
[4] McClure J W 1957 Band structure of graphite and de Haas–van Alphen effect *Phys. Rev.* **108** 612–8
[5] Slonczewski J C and Weiss P R 1958 Band structure of graphite *Phys. Rev.* **109** 272–9
[6] Haering R R 1958 Band structure of rhombohedral graphite *Can. J. Phys.* **36** 352–62
[7] McClure J W 1969 Electron energy band structure and electronic properties of rhombohedral graphite *Carbon* **7** 425–32
[8] Painter G S and Ellis D E 1970 Electronic band structure and optical properties of graphite from a variational approach *Phys. Rev.* B **1** 4747–52
[9] Tománek D and Louie S G 1988 First-principles calculation of highly asymmetric structure in scanning-tunneling-microscopy images of graphite *Phys. Rev.* B **37** 8327–36
[10] Charlier J-C, Gonze X and Michenaud J-P 1991 First-principles study of the electronic properties of graphite *Phys. Rev.* B **43** 4579–89
[11] Novoselov K S, Geim A K, Morozov S V, Jiang D, Zhang Y, Dubonos S V, Grigorieva I V and Firsov A A 2004 Electric field effect in atomically thin carbon films *Science* **306** 666
[12] Latil S and Henrard L 2006 Charge carriers in few-layer graphene films *Phys. Rev. Lett.* **97** 036803
[13] Partoens B and Peeters F M 2006 From graphene to graphite: electronic structure around the k point *Phys. Rev.* B **74** 075404
[14] Partoens B and Peeters F M 2007 Normal and dirac fermions in graphene multilayers: tight-binding description of the electronic structure *Phys. Rev.* B **75** 193402
[15] Guinea F, Castro A H Neto and Peres N M R 2006 Electronic states and Landau levels in graphene stacks *Phys. Rev.* B **73** 245426
[16] Avetisyan A A, Partoens B and Peeters F M 2010 Stacking order dependent electric field tuning of the band gap in graphene multilayers *Phys. Rev.* B **81** 115432
[17] Yuan S, Roldán R and Katsnelson M I 2011 Landau level spectrum of *ABA*- and *ABC*-stacked trilayer graphene *Phys. Rev.* B **84** 125455
[18] Taychatanapat T, Watanabe K, Taniguchi T and Jarillo-Herrero P 2011 Quantum Hall effect and Landau-level crossing of Dirac fermions in trilayer graphene *Nature Phys.* **7** 621–5
[19] Yuan S, Roldán R and Katsnelson M I 2011 Excitation spectrum and high-energy plasmons in single-layer and multilayer graphene *Phys. Rev.* B **84** 035439
[20] Zhang F, Min H, Polini M and MacDonald A H 2010 Spontaneous inversion symmetry breaking in graphene bilayers *Phys. Rev.* B **81** 041402
[21] Zhang F, Jung J, Fiete G A, Niu Q and MacDonald A H 2011 Spontaneous quantum Hall states in chirally stacked few-layer graphene systems *Phys. Rev. Lett.* **106** 156801
[22] Nandkishore R and Levitov L 2010 Quantum anomalous Hall state in bilayer graphene *Phys. Rev.* B **82** 115124
[23] Lemonik Y, Aleiner I L and Fal'ko V I 2012 Competing nematic, anti-ferromagnetic and spin-flux orders in the ground state of bilayer graphene arXiv:1203.4608

[24] Zhang F and MacDonald A H 2011 Distinguishing spontaneous quantum Hall states in graphene bilayers arXiv:1107.4727
[25] Weitz R T, Allen M T, Feldman B E, Martin J and Yacoby A 2010 Broken-symmetry states in doubly gated suspended bilayer graphene *Science* **330** 812–6
[26] Bao W *et al* 2011 Stacking-dependent band gap and quantum transport in trilayer graphene *Nature Phys.* **7** 948–52
[27] Velasco J *et al* 2012 Transport spectroscopy of symmetry-broken insulating states in bilayer graphene *Nature Nanotechnol.* **7** 156–60
[28] Mayorov A S *et al* 2011 Interaction-driven spectrum reconstruction in bilayer graphene *Science* **333** 860–3
[29] Zhang F, Sahu B, Min H and MacDonald A H 2010 Band structure of *abc*-stacked graphene trilayers *Phys. Rev.* B **82** 035409
[30] Trushin M and Schliemann J 2011 Pseudospin in optical and transport properties of graphene *Phys. Rev. Lett.* **107** 156801
[31] Jung J, Zhang F and MacDonald A H 2011 Lattice theory of pseudospin ferromagnetism in bilayer graphene: competing interaction-induced quantum Hall states *Phys. Rev.* B **83** 115408
[32] Min H, Borghi G, Polini M and MacDonald A H 2008 Pseudospin magnetism in graphene *Phys. Rev.* B **77** 041407
[33] Nair R R, Blake P, Grigorenko A N, Novoselov K S, Booth T J, Stauber T, Peres N M R and Geim A K 2008 Fine structure constant defines visual transparency of graphene *Science* **320** 1308
[34] Karch J *et al* 2008 Photon helicity driven electric currents in graphene arXiv:1002.1047
[35] Juri L O and Tamborenea P I 2008 Hartree–Fock ground state of the two-dimensional electron gas with Rashba spin–orbit interaction *Phys. Rev.* B **77** 233310
[36] Jang C, Adam S, Chen J-H, Williams E D, Das Sarma S and Fuhrer M S 2008 Tuning the effective fine structure constant in graphene: opposing effects of dielectric screening on short- and long-range potential scattering *Phys. Rev. Lett.* **101** 146805
[37] Peres N M R, Guinea F and Castro Neto A H 2005 Coulomb interactions and ferromagnetism in pure and doped graphene *Phys. Rev.* B **72** 174406
[38] Nandkishore R and Levitov L 2011 Polar Kerr effect and time reversal symmetry breaking in bilayer graphene *Phys. Rev. Lett.* **107** 097402
[39] Thouless D J, Kohmoto M, Nightingale M P and den Nijs M 1982 Quantized Hall conductance in a two-dimensional periodic potential *Phys. Rev. Lett.* **49** 405–8
[40] Hasan M Z and Kane C L 2010 Colloquium: topological insulators *Rev. Mod. Phys.* **82** 3045–67
[41] Kane C L and Mele E J 2005 Quantum spin Hall effect in graphene *Phys. Rev. Lett.* **95** 226801
[42] Prada E, San-Jose P, Brey L and Fertig H A 2011 Band topology and the quantum spin Hall effect in bilayer graphene *Solid State Commun.* **151** 1075–83
[43] Xiao D, Yao W and Niu Q 2007 Valley-contrasting physics in graphene: magnetic moment and topological transport *Phys. Rev. Lett.* **99** 236809
[44] Mucha-Kruczyński M, Aleiner I L and Fal'ko V I 2011 Strained bilayer graphene: band structure topology and Landau level spectrum *Phys. Rev.* B **84** 041404